Combust. Sci. and Tech., 177: 89–106, 2005

ISSN: 0010-2202 print/1563-521X online
DOI: 10.1080/00102200590883769

Taylor & Francis
Taylor & Francis Group

BURNING VELOCITIES AND A HIGH-TEMPERATURE SKELETAL KINETIC MODEL FOR *n*-DECANE

ZHENWEI ZHAO, JUAN LI, ANDREI KAZAKOV, AND FREDERICK L. DRYER*

Department of Mechanical and Aerospace Engineering,
Princeton University, Princeton,
New Jersey, USA

STEPHEN P. ZEPPIERI

United Technologies Research Center,
East Hartford, Connecticut, USA

Laminar flame speeds of *n*-decane/air mixtures were determined experimentally over an extensive range of equivalence ratios at 500 K and at atmospheric pressure. The effect of N_2 dilution on the laminar flame speed was also studied at these same conditions. The experiments employed the stagnation jet–wall flame configuration with the flow velocity field determined by particle image velocimetry. Reference laminar flame speeds were obtained using linear extrapolation from low to zero stretch rate. The determined flame speeds are significantly different from those predicted using existing published kinetic models, including a model validated previously against high-temperature data from flow reactor, jet-stirred reactor, shock tube ignition delay, and burner-stabilized flame experiments. A significant update of this model is described

Received 26 April 2004; accepted 2 June 2004.

This work was supported by NASA under COOP NCC3-735 and by the Chemical Sciences, Geosciences and Biosciences Division, Office of Basic Energy Sciences, Office of Science, U.S. Department of Energy under Grant No. DE-FG02–86ER13503. The technical contributions of Dr. Michele Angioletti and Mr. Paul Michniewicz in performing the experiments, and of Mr. Kenneth Kroenlein in performing the model analysis, are also acknowledged.

*Address correspondence to fldryer@princeton.edu

that continues to predict the earlier validation experiments as well as the newly acquired laminar flame speed data and other recently published shock-tube ignition delay measurements.

Keywords: skeletal reduced kinetic model, *n*-decane, burning velocity, premixed flame, dilution

INTRODUCTION

Improving internal combustion engine efficiency (to control CO_2 production) while continuing to minimize combustion pollutant emissions requires increased emphasis on more accurate numerical design tools for internal combustion engine development. Robust chemical kinetics models are needed to predict the complex physical and chemical processes that occur in advanced engine designs that utilize distillate-type fuels; for example, direct-injection diesel and homogeneous charge compression ignition operation. Because practical diesel fuels are complex mixtures of very large numbers of different hydrocarbon species, extensive efforts have been focused on understanding and numerically modeling single components and simple mixtures of components that emulate diesel fuel autoignition and combustion properties. In multidimensional engine simulations, it is not currently possible to use detailed hydrocarbon models involving large numbers of reactions and species. Recognizing the problem of mechanistic complexity versus predictive robustness, our laboratory previously developed a partially reduced skeletal mechanism approach for high-temperature, large *n*-alkane oxidation and pyrolysis by applying the methodology to *n*-decane (Zeppieri et al., 2000a). In the kinetic model, the number of required species was significantly reduced by using a novel method of assumption that each of the *n*-alkyl radicals with more than three carbon atoms is in isomeric partial equilibrium. Constructs with carbon number of three or fewer were simulated using detailed elementary kinetics. The resulting *n*-decane kinetic model was shown to reproduce high-temperature atmospheric pressure flow reactor pyrolysis and oxidation (Zeppieri et al., 2000a), jet-stirred reactor oxidation (Bales-Gueret et al., 1992), and shock-tube ignition delay data (Pfahl et al., 1996). In presenting the published paper (Zeppieri et al., 2000b), predictions were also shown to compare favorably with the burner-stabilized flame data of Douté et al. (1995). However, no comparisons were made with laminar flame speed data, primarily because only two

data points from high-temperature Bunsen burner experiments were available in the literature (Wagner and Dugger, 1955). Furthermore, only one point obtained by extrapolation of these data to room temperature and atmospheric pressure has typically been used for comparison. More recently, Bikas and Peters (2001) published a kinetic model for *n*-decane oxidation and compared predictions with this single extrapolated measurement. The most recent *n*-decane laminar speed data were reported by Skjøth-Rasmussen et al. (2003). As in the early experiments, Skjøth-Rasmussen et al. utilized the Bunsen burner approach for determining the flame speed, and no stretch corrections were applied to the measurements.

The laminar flame speed (i.e., the propagation speed of a one-dimensional, adiabatic, planar, laminar flame in a doubly infinite domain) embodies the fundamental properties of diffusivity, reactivity, and exothermicity for a given mixture and is commonly used to partially validate kinetic models. As noted earlier, the literature is sparse for accurate laminar flame speed data for *n*-decane, and this is also more generally true for all higher-molecular-weight species characteristic of gas-turbine and diesel fuel components. Thus, additional experimental laminar flame speed data are important to advancing comprehensive kinetic models for large-carbon-number species that can be utilized in developing smaller-dimensional models for design applications involving diesel as well as gas-turbine energy conversion systems.

The specific objective of the present work was to experimentally determine laminar flame speeds of *n*-decane/air mixtures over a range of equivalence ratio at 500 K, with particular interest near lean flammability and sooting limit conditions. Because applications frequently involve exhaust-gas recirculation, the dilution effect on the laminar flame speed was also studied for a range of equivalence ratios with N_2 dilution volume percentages up to 20%. The generated data were then compared with the predictions using kinetic models appearing in the literature (Bikas and Peters, 2001; Zeppieri et al., 2000a). In collaboration with Bikas and Peters (2001), we were unable to reproduce the calculations shown in the original paper. Disparity was also found in comparison with predictions utilizing the model reported by Zeppieri et al. (2000a). Here, we update the latter model with modifications in submechanisms, elementary rate parameters, and thermochemistry and compare the updated mechanism with the new laminar flame speed data, and well as other data appearing in the literature.

EXPERIMENTAL METHODOLOGY

The single jet–wall stagnation flame experimental configuration for determining laminar flame speeds was first introduced by Egolfopoulos et al. (1997), and the basic single jet–wall stagnation flame technique and the modified procedural methodologies we use in our laboratory are discussed in more detail elsewhere (Zhao, 2002). A premixed reactant flow emerges vertically upward from the 14-mm converging nozzle situated at the center of a water/N_2-cooled burner surface and impinges vertically onto an 8-cm-diameter thin ceramic, flat, stagnation plate (Figure 1). When the strain rate is low, the flame front is far away from the (nearly) adiabatic stagnation plate; therefore, the small downstream heat loss has minimal effect on the flame propagation speed. The burner flow is shrouded by a 2-mm annular flow of nitrogen to stabilize the core flame.

A metered airflow is first seeded with 0.3–0.7-micron boron nitride particles to apply Particle Image Velocity (PIV), and then the particle-laden flow is preheated using an inline heater. The flow is then mixed with preheated, prevaporized fuel in a turbulent mixer. The residence time of fully mixed components upstream of the burner is restricted to preheat temperatures that do not lead to two-stage ignition/flashback conditions.

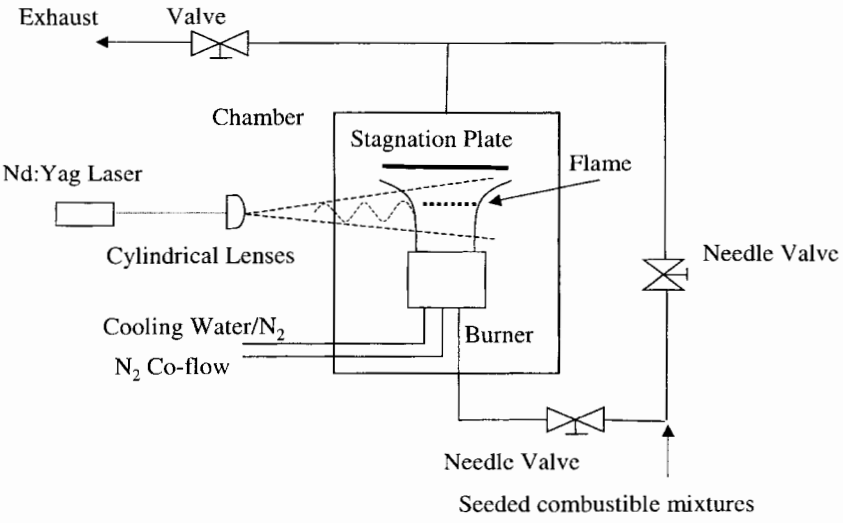

Figure 1. Schematics of the experimental setup.

The flow of particle-laden, premixed mixture is then separated into two parts by a pressure drop across two high-temperature needle valves. By varying the relative pressure drop of the two flow channels, the core flow rate to the burner and that purged directly to exhaust can be varied to change the burner flow velocity without manipulating the individual flow rates of each component (which can be a source of uncertainty in maintaining experimental equivalence ratio). The N_2 shroud coflow is independently heated and temperature controlled to match the temperature of the entering burner flow, and all of the gas heaters, mixer, and needle flow splitters are installed in an insulated container to maintain near-isothermal conditions. The burner body itself is also heated and independently temperature controlled. Several 1.6-mm exposed-junction fast-response thermocouples are used to monitor local temperatures. The final temperature of the burner flow, which is measured 3.8 mm upstream of and prior to a screen at the burner nozzle exit plane, is used as the control temperature. The location of the temperature sensor was selected to minimize flame radiation effects and flow disturbance and to achieve close proximity to the flame location itself.

A Continuum® Minilite PIV Nd:Yag laser is used as the PIV light source and the light beam is shaped into a thin light sheet using cylindrical and spherical lenses. The images at two different times are recorded by double exposure using a Kodak DCS 460 digital camera with resolution of 3060×2036 pixels. The recorded images, in appropriate digital form, are subsequently analyzed using an in-house autocorrelation code. The PIV code utilizes self-optimizing fast Fourier transform algorithms, variable interrogation window size, and subpixel peak-detection techniques. In addition, customized filtering algorithms implemented in the code facilitate autodetection of the flow centerline and the flame edge, allowing the processing of large data sets (reducing statistical experimental errors) with minimal user interaction. Additional features include algorithms for automatic interrogation peak selection/rejection as well as stretch rate/reference flame speed determination. The use of this software package eliminates human bias in determining the stretch rate manually, which is a technique commonly reported for the laser Doppler velocimetry/PIV-related flame speed studies appearing in the literature.

PIV was employed to velocity-map the entire two-dimensional flow field for each set of experimental conditions. The particle density and displacement between two exposures were chosen for optimal application

of the autocorrelation technique. Because of thermal expansion and flow acceleration upstream of the flame front, the particle density becomes too low to obtain reliable vectors using autocorrelation at the flame front itself. However, the rapid particle acceleration and loss of correlation results in a very well-defined flame front location (Hirasawa et al., 2002; Zhao 2002). The minimum velocity location in the axial velocity profile was defined as the reference flame speed, while the stretch rate for each measurement was determined from the quasi-linear part of the axial velocity profile upstream. Linear extrapolation was used to determine the zero-stretched laminar flame speed from a plot of the reference flame speed versus the stretch rate. The direction of the velocity in a stagnation flow is well defined, thus avoiding a directional ambiguity issue characteristic of the autocorrelation approach.

RESULTS AND DISCUSSION

The vapor-pressure temperature dependence of *n*-decane is such that, at atmospheric pressure, no flammable vapor/air ratios can be formed at room temperature. To perform flame speed measurements over a wide range of stoichiometry, the present experiments (Figure 2) were performed at atmospheric pressure and with the mixtures preheated to an initial temperature of 500 K. Experiments were conducted with and without additional N_2 dilution of the mixture to simulate the effects of exhaust-gas recirculation on laminar flame speed. The dilution ratio is defined here as the mole fraction of the diluent in the total mixture (diluent + air + fuel) expressed as a percentage.

The statistical averaging of the raw experimental data can reduce the uncertainties in the measured flame velocities and stretch rates. Uncertainties in stretch rate are one of the largest sources of error determining laminar flame speeds using the stagnation flame method (Zhao, 2002). Although the automatic determination of the stretch rate used in the present work is more systematic, it may result in an apparent greater degree of scatter, which would otherwise appear smaller as a result of human bias present in manual data reduction. In the present work, the uncertainty in the equivalence ratio is about ± 0.01. The uncertainty in the determined flame speed evaluated using conventional regression analysis is less than about 5% (Zhao et al., 2004b).

The laminar flame speed data obtained in the present work are also consistent with the experimental data of Wagner and Dugger (1955).

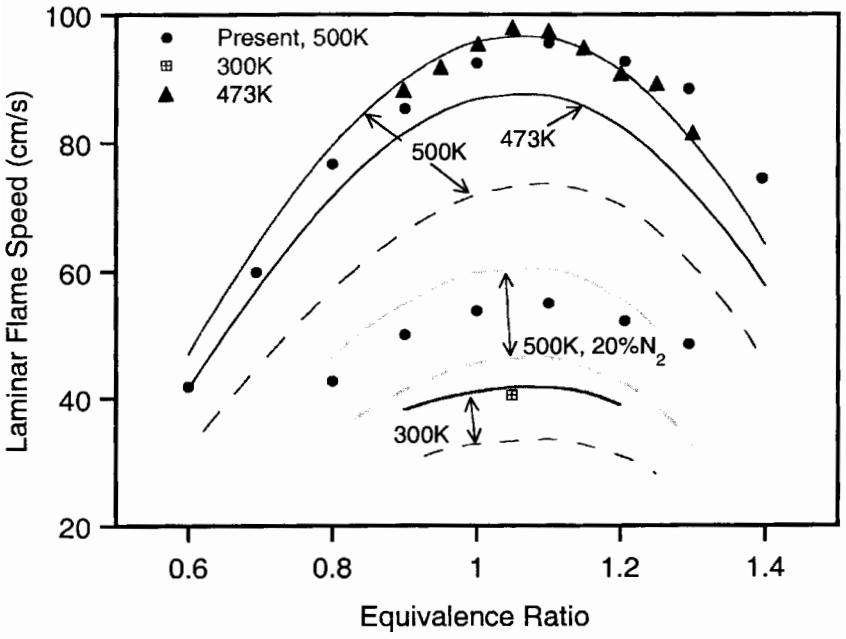

Figure 2. Atmospheric pressure laminar flame speeds for *n*-decane/air mixtures. Symbols: 500 K and 500 K with 20% N_2 dilution, present experimental data; 300 K, Wagner and Dugger (1955) (extrapolated based on two higher temperature measurements); 473 K, Skjøth-Rasmussen et al. (2003); lines: model predictions (dashed line, Zeppieri et al., 2000a; solid line, present *n*-decane model).

Using their temperature extrapolation correlation, $U_f = cT_0^a$, where T_0 is the initial temperature, c and a are empirical constants (for *n*-decane at $\varphi = 1.05$, $c = 1.67$, $a = 2.97 \times 10^{-3}$), we obtain the value of 95.5 cm/s at 500 K. Our experimental measurements at $\varphi = 1.05$ for the case without dilution yield 94.0 cm/s, and the difference is well within the accuracy of the experiments and the correlation itself.

Laminar flame speed predictions were obtained using PREMIX (Kee et al., 1985) and CHEMKIN II packages (Kee et al., 1989a). Transport parameters were taken from the Sandia database (Kee et al., 1989b), and unknown Lennard–Jones parameters were estimated from the species critical properties using techniques described by Wang and Frenklach (1994). Critical properties (T_c and P_c) were also estimated using the group contribution approach of Joback (Reid et al., 1987), as implemented in the NIST software package (Stein, 1994).

Predictions using the kinetic models of Zeppieri et al. (2000) and Bikas and Peters (2001) were compared with the experimental results. Figure 2 shows the comparison of predictions using the Zeppieri et al. model with the single experimental point at 300 K used previously by Bikas and Peters and with our new experimental data at 500 K. The Zeppieri et al. model significantly underpredicts the experimentally determined peak flame speeds. Calculations using the Bikas and Peters model from the thesis of Bikas (2001) or the publication underpredict the experimental results by similar magnitudes. However, the Bikas – Peters model also predicts flame speeds that differ substantially from those reported in the original paper. Peters and colleagues have collaborated with us in an attempt to resolve these discrepancies (Honnet and Peters, personal communication, 2003). While it has been mutually concluded that our implementation of the kinetics and calculations are indeed correct, the source of the discrepancy from the published results remains unresolved.

Since the development of the original Zeppieri et al. model, significant advances in fundamentals (mechanistic issues, thermochemical and kinetic parameters) have occurred, particularly for H_2/O_2 and C_1–C_3 kinetics. As a result, we investigated and updated the small molecule and radical kinetics and thermochemistry utilized in the Zeppieri et al. model to evaluate recent updates on the predicted laminar flame speeds. In particular, we revised the model by substituting our recent update of the H_2/O_2 kinetic model (Li et al, 2004). The key updates included new expressions for the $H + O_2 = OH + O$ (Hessler, 1998) and $H + O_2 + M = HO_2 + M$ (Michael et al., 2002) reactions, a revision in the heat of formation of OH radical (Ruscic et al., 2002), and a modification of the rate expression utilized for $H + OH + M$ (Li et al, 2004) (which appears to contribute primarily to achieving good agreement with high-pressure laminar flame speed data).

The C_1–C_3 kinetics in the model were replaced with those recently published by Qin et al. (2000), with the following modifications:

1. $aC_3H_5 + HO_2 \rightarrow OH + C_2H_3 + CH_2O$. Similar to the recent work of Zheng et al. (2003), this global reaction was first replaced with the corresponding elementary step, $aC_3H_5 + HO_2 = OH + C_3H_5O$ (R_1). The new intermediate species, C_3H_5O, was introduced into the mechanism and the associated thermochemical data were estimated using the THERM package (Ritter and Bozzelli, 1991). The reaction

rate was taken to be the same as that for the global reaction. Also, the decomposition reactions of C_3H_5O, $C_3H_5O = C_2H_3 + CH_2O$ (R_2) and $C_3H_5O = C_2H_3CHO + H$ (R_3) were added to the mechanism. Rate coefficient of reactions (R_2) and (R_3) were estimated using kinetic information for similar reactions available in the literature (Baulch et al., 1994; Wang et al., 1999).

2. The rate coefficient of $CH_3 + X$ reactions was replaced by that reported by Scire et al. (2001).

The complete mechanism used in this study may be obtained electronically by contacting the corresponding author.

The predictions utilizing the updated model (Figure 2) agree well with the newly, obtained flame speed data, especially for the fuel-lean and stoichiometric results. A small discrepancy still remains on the fuel-rich side. The prediction for diluted flame speed conditions also agree reasonably well with the experimental data. Although it is possible to further improve the agreement between the model predictions and the present data by adjusting less-established rate coefficients or thermochemistry within known uncertainties, uncertainty contributions may also come from other sources such as the transport model (Kee et al., 1989b). Figure 2 also shows the *n*-decane flame speeds at initial temperature of 473 K reported by Skjøth-Rasmussen et al. (2003). The data essentially overlap the present experimental data obtained at a higher initial temperature of 500 K. Moreover, the present model well predicts the present and other published data obtained at both higher and lower initial temperatures than that of the Skjøth-Rasmussen et al. data. The sources of the discrepancy of Skjøth-Rasmussen et al. is data with our data certainly include the fact that the reported results were not corrected for stretch but may include other unknown sources.

To illustrate the influence of individual reaction rates on predicted flame speeds, a sensitivity analysis was performed for three selected cases of lean, stoichiometric, and rich mixture compositions at 500 K without N_2 dilution using the Zeppieri et al. model. The sensitivity spectra at the same conditions with N_2 dilution are very similar to that without dilution, and only those without dilution are presented in Figure 3.

The sensitivity spectrum for *n*-decane/air flames exhibits features typically observed previously and well documented for flames of small- (e.g., see Qin et al., 2000; Smith et al., 1999) as well as larger-molecular-weight (e.g., see Held et al., 1997) alkanes. The sensitivity spectrum is

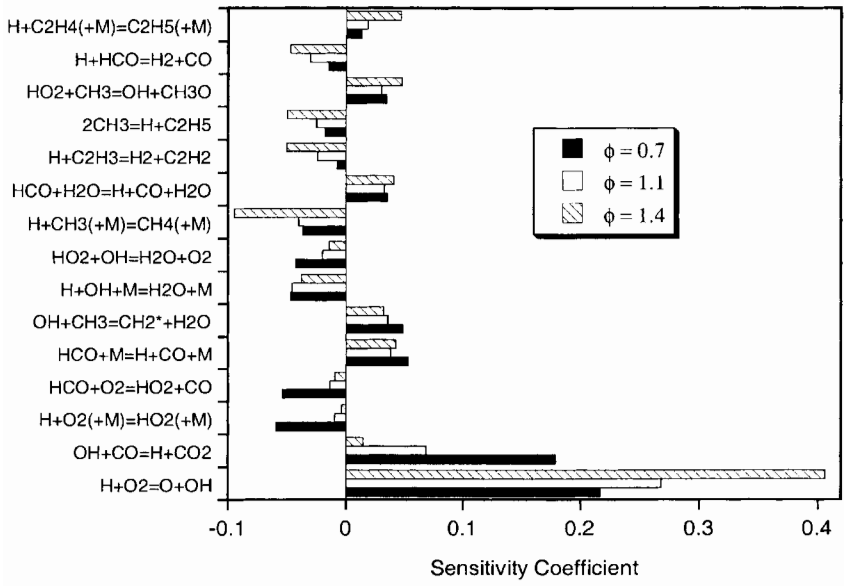

Figure 3. Normalized sensitivity coefficients of *n*-decane flame speeds at 500 K calculated using the present kinetic model.

dominated by the main chain-branching reaction, $H + O_2 = OH + O$, CO oxidation, $CO + OH = CO_2 + H$, the reactions of formyl radical, particularly $HCO + M = CO + H + M$ and $HCO + O_2 = CO + HO_2$, and several C_2 and C_3 reactions. Reactions involving the fuel itself or species larger than C_4 produced during the oxidation make no significant contribution to the predicted flame speed. The latter observation points to the lack of utility of using flame speed values to validate large-molecule (and high-molecular weight-fragments) kinetic chemistry. All of the preceding factors as well as the literature suggest that the inadequacy in predicting flame speeds of large-carbon-number fuels is related to the inadequacies of the small-species kinetics.

We further investigated the ability of the revised model to reproduce the data compared against the original Zeppieri et al. model as well as with other data. The agreement of the revised model with the pyrolysis data presented by Zeppieri et al. (2000b) shown in Figure 4, is essentially of similar quality as that achieved with the Zeppieri et al. model for major species and intermediates (e.g., *n*-decane, ethane, ethene, methane, and propene) and remains less satisfactory for trace intermediates (e.g.,

1,3-butadiene, pentene). Comparisons with the *n*-decane oxidation data of in Zeppieri et al. (2000a) are similarly in good agreement with earlier results, with the some disparities still remaining for CO and 1,3-butadiene (Figure 5). The sensitivity analysis performed for the flow reactor conditions suggest the need for further model refinement for reactions involving both pentene and 1,3-butadiene, such as $C_5H_{10} + OH = H_2O + C_4H_6 + CH_3$, as well as in the submechanism at the C_3 level.

Model predictions were also compared with the published burner-stabilized flame data of Douté et al. (1995). As shown in Figure 6, the model reproduces the observed fuel/O_2 decay and the major species evolution (e.g., H_2O, CO_2, C_3H_6) very well, with some slight discrepancies for minor species such as CO and 1,3-butadiene.

Finally, the present data were also validated against shock-tube ignition delay data that recently appeared in the literature (Horning et al., 2002; Figure 7). Constant-volume, zero-dimensional adiabatic conditions were used in these simulations, and the computed ignition delay time was determined from CH radical peak or pressure rise, consistent with the experimental measurement methods. The predicted ignition delays are in excellent agreement with 1.2-atm, high-temperature cases (Horning et al., 2002).

Comparisons with the high-pressure ignition delay data (Pfahl et al., 1996) are also very good at high temperatures, but discrepancies become substantial below 1100 K. This disagreement is expected because the high-temperature mechanism utilized here does not include radical-oxygen addition reactions characteristic of low- and intermediate-temperature oxidation of large-carbon-number species.

CONCLUSIONS

Laminar flame speeds for *n*-decane/air mixtures at atmospheric pressure and initial temperature of 500 K were determined on a stagnation flame burner using PIV. Predictions of the experimental data based on the partially reduced skeletal mechanism for *n*-decane pyrolysis and oxidation by Zeppieri et al. (2000a) were found to be in poor agreement. The analyses of these results further support that laminar flame speed data for large-carbon-number alkanes primarily constrains the kinetic submechanisms for hydrogen/carbon monoxide oxidation and small-carbon-containing species with carbon number generally less than 3. Revision of the Zeppieri et al. model by updating the hydrogen/oxygen and small-carbon-number C_1–C_3 submechanisms, thermochemistry, and elementary rates results in acceptable

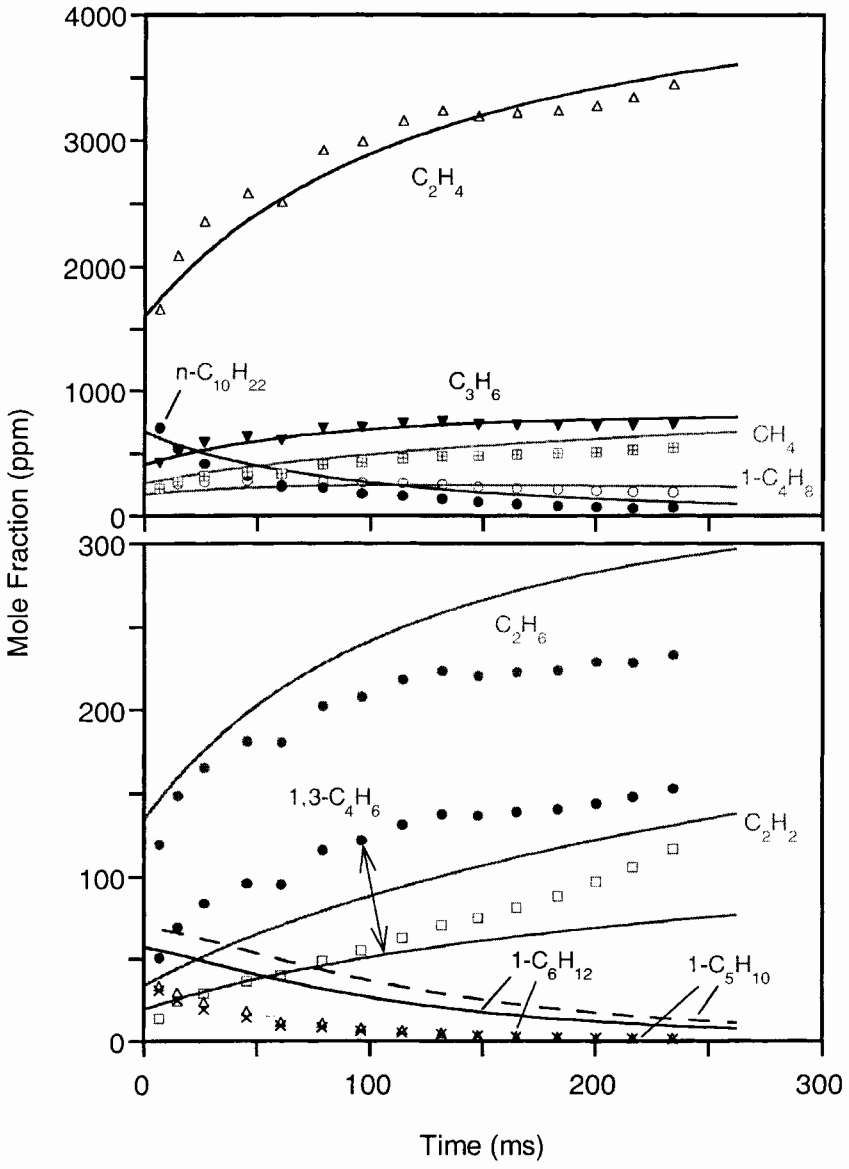

Figure 4. Comparison of experimental (Zeppieri et al., 2000a) (symbols) and computed (lines) species profiles during *n*-decane pyrolysis in a flow reactor ($P = 1$ atm, $T_i = 1060$ K, initial *n*-decane concentration 1456 ppm in N_2). Model predictions are shifted by 46 ms.

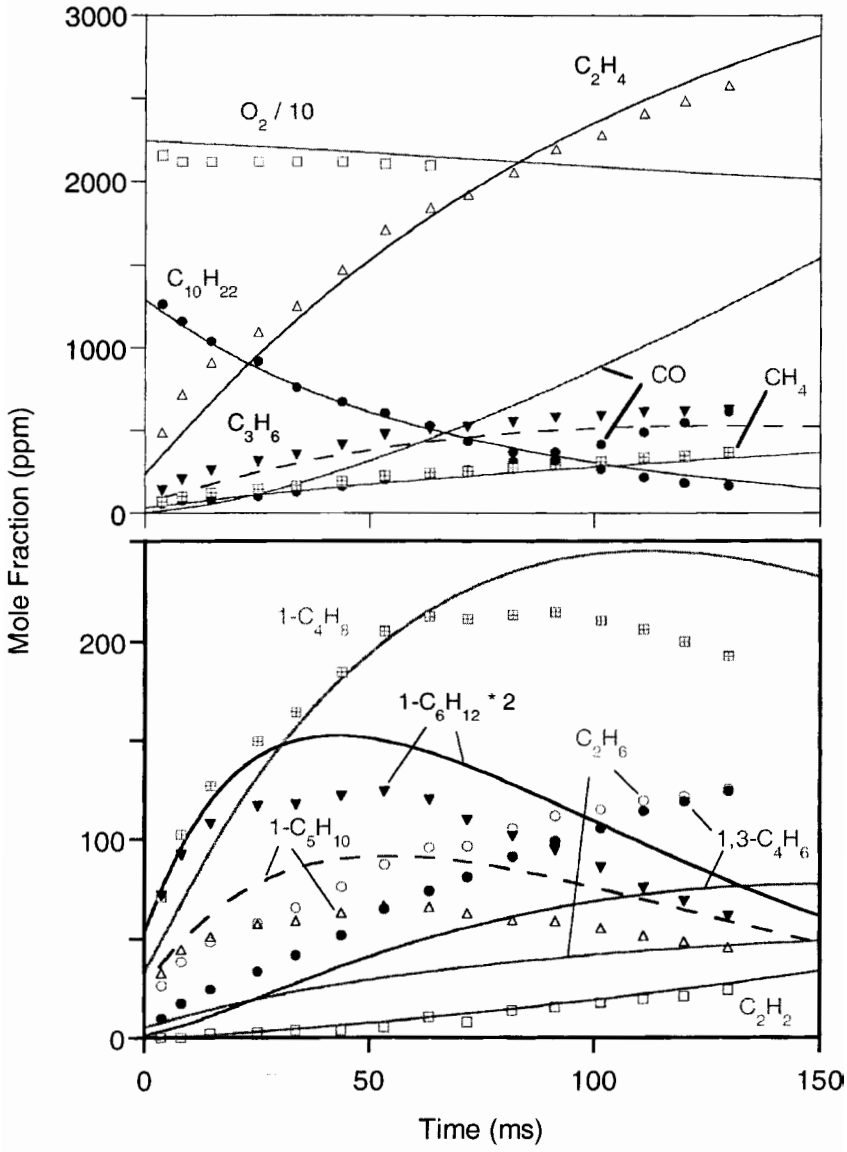

Figure 5. Comparison of experimental (Zeppieri et al., 2000a) (symbols) and computed (lines) species profiles during *n*-decane oxidation in a flow reactor ($P = 1$ atm, $T_i = 1019$ K, $\phi \approx 1.0$, initial *n*-decane concentration 1452 ppm in N_2). Model predictions are shifted by 11.6 ms.

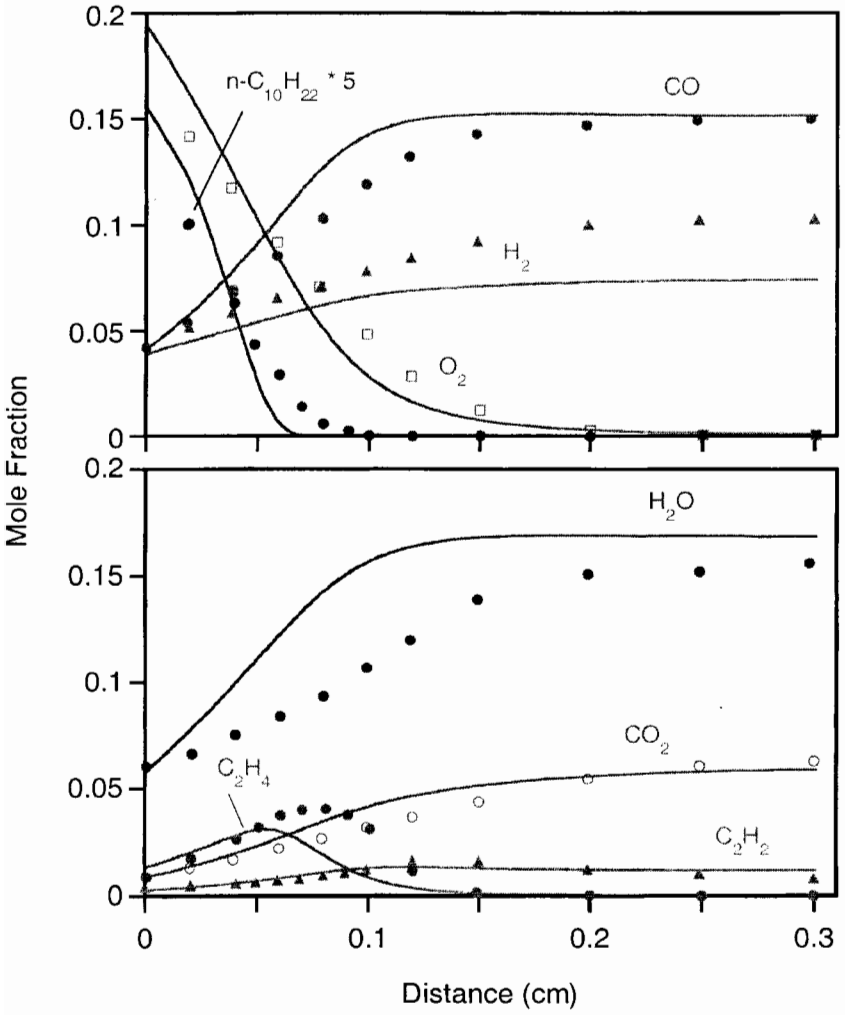

Figure 6. Comparison of experimental (Doute et al. 1995) (symbols) and computed (lines) species profiles in *n*-decane/O_2/N_2 burner stabilized flame ($P = 1$ atm, $\phi = 1.7$).

prediction of the experimental results. Predictions using the revised model were found to reproduce data used in validating the original model by Zeppieri et al. (2000a) including high-temperature, atmospheric pressure flow reactor pyrolysis and oxidation, high-pressure shock-tube ignition delay, and stirred reactor species measurements. The revised model predic-

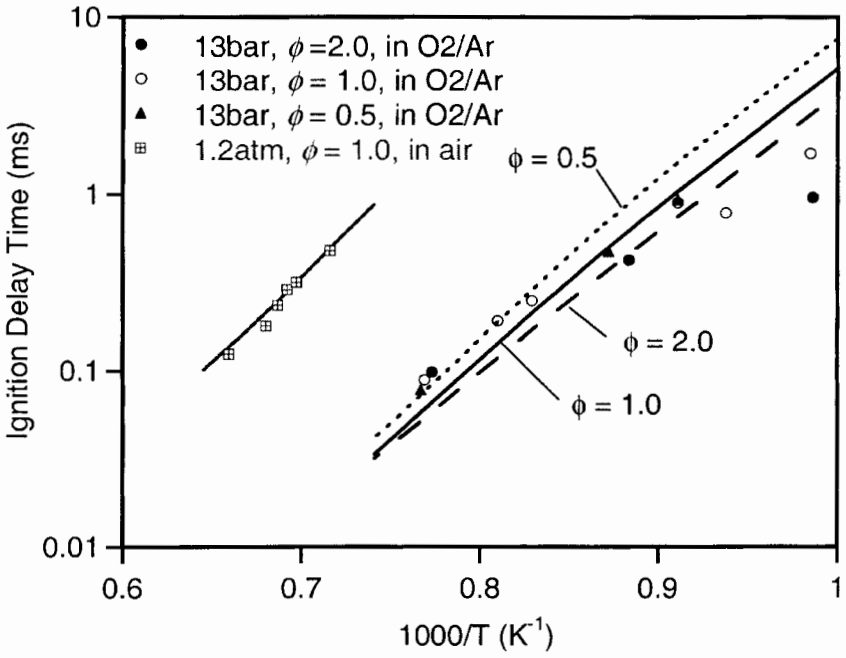

Figure 7. Comparison of experimental (symbols) and computed (lines) ignition delay times for *n*-decane. Mixture composition used in the experiments: 0.2% *n*-decane/O_2/Ar (Horning et al., 2002) and *n*-decane/air (Pfahl et al., 1996).

tions also agree well with atmospheric-pressure, burner-stabilized flame data and recently published shock-tube ignition delay measurements at both low and high pressure.

As noted earlier, the present mechanism is developed for high-temperature applications where the reactions of radicals with oxygen that are of significance to two-stage ignition phenomena are not of importance. Recent work in our laboratory on kinetic modeling of two-stage large-alkane oxidation suggests that without first developing robust high-temperature mechanistic features, the resulting coupling precludes construction of predictive models for low-and intermediate-temperature kinetics. Addition of low- and intermediate-temperature submechanisms to the present high-temperature mechanism is the subject of current work in our laboratory and will result in a wide-ranged mechanism for *n*-decane oxidation for applications involving two-stage ignition as well as high-temperature oxidation phenomena.

REFERENCES

Bales-Gueret, C., Cathonnet, M. Boettner, J.-C., and Gaaillard, F. (1992) Experimental-study and IEIC modeling of higher hydrocarbons oxidation in a jet-stirred flow reactor. *Energy Fuels*, **6**, 189.

Baulch, D.L., Cobos, C.J., Cox, R.A., Esser, C., Frank, P., Just, Th., Kerr, J.A., Pilling, M.J., Troe, J., Walker, R.W., and Warnatz, J. (1994) CEC group on evaluation of kinetic data for combustion modeling. *J. Phys. Chem. Ref. Data*, **23**, 847.

Bikas, G. (2001) Kinetic mechanisms for hydrocarbon ignition, Ph. D. Thesis. Institut fur Technische Mechanik, RWTH Aachen, Germany.

Bikas, G. and Peters, N. (2001) Kinetic modeling of n-decane combustion and autoignition. *Combust. Flame*, **126**, 1456.

Doute, C., Delfau, J.L., Akrich, R., and Vovelle, C. (1995) Chemical structure of atmospheric pressure premixed *n*-decane and kerosene flames. *Combust. Sci. Technol.*, **106**, 327.

Egolfopoulos, F.N., Zhang, H., and Zhang, Z. (1997) Wall effects on the propagation and extinction of steady, strained, laminar premixed flames. *Combust. Flame*, **109**, 237.

Held, T.J., Marchese, A.J., and Dryer, F.L. (1997) A semi-empirical reaction mechanism for *n*-heptane oxidation and pyrolysis. *Combust. Sci. Technol.*, **123**, 107.

Hessler, J.P. (1998) Calculation of reactive cross sections and microcanonical rates from kinetic and thermochemical data. *J. Phys. Chem. A*, **102**, 4517.

Hirasawa, T., Sung, C.J., Joshi, A., Yang, Z., Wang, H., and Law, C.K. (2002) Determination of Laminar Flame Speeds Using Digital Particle Image Velocimetry: Binary Fuel Blends of Ethylene, n-Butane, and Toluene, *Proc. Combust. Instit.*, **29**, 1427.

Horning, D.C., Davidson, D.F., and Hanson, R.K. (2002) Study of the high-temperature autoignition of n-alkane/O_2/Ar mixtures. *J. Propul. Power*, **18**, 363.

Kee, R.J., Grcar, J.F., Smooke, M.D., and Miller, J.A. (1985) *A Fortran Program for Modeling Steady Laminar One-Dimensional Premixed Flames*. Sandia Report SAND85–8240, Sandian National Laboratories, Albuquerque, NM.

Kee, R.J., Rupley, F.M., and Miller, J.A. (1989a) *CHEMKIN II: A Fortran Chemical Kinetics Package for the Analysis of Gas Phase Chemical Kinetics*. Sandia Report SAND89–8009, Sandia National Laboratories, Albuquerque, NM.

Kee, R.J., Dixon-Lewis, J., Warnatz, J. Coltrin, J.A., and Miller, J.A. (1989b) *A Fortran Computer Code for the Evaluation of Gas Phase, Multicomponent Transport Properties*. Sandia Report SAND86–8284, Sandia National Laboratories, Albuquerque, NM.

Li, J., Zhao, Z., Kazakov, A., and Dryer, F.L. (2004) An updated comprehensive kinetics model of H_2 combustion. *Int. J. Chem. Kinet.*, **36**, 566.

Michael, J.V., Su, M.C., Sutherland, J.W., Carroll, J.J., and Wagner, A.F. (2002) Rate constants for $H+O_2+M \rightarrow HO_2+M$ in seven bath gases. *J. Phys. Chem. A*, **106**, 5297.

Pfahl, U., Fieweger, K., and Adomeit, G. (1996) Self-Ignition of Diesel-Relevant Hydrocarbon-Air Mixtures under Engine Conditions, *Proc. Combust. Instit.*, **26**, 781.

Qin, Z., Lissianski, V., Yang, H., Gardiner, W.C., Jr., Davis, S.G., and Wang, H. (2000) Combustion chemistry of propane: A case study of detailed reaction mechanism optimization, *Proc. Combust. Instit.*, **28**, 1663.

Reid, R.C., Prausnitz, J.M., and Poling B.E. (1987) *The Properties of Gases and Liquids*, 4th ed., McGraw-Hill, New York.

Ritter, E.R. and Bozzelli, J.W. (1991) THERM—Thermodynamic property estimation for gas-phase radicals and molecules. *Int. J. Chem. Kinet.*, **23**, 767.

Ruscic, B., Wagner, A.F., Harding, L.B., Asher, R.L., Feller, D., Dixon, D.A., Peterson, K.A., Song, Y., Qian, X.M., Ng, C.Y., Liu, J.B., and Chen, W.W. (2002) On the enthalpy of formation of hydroxyl radical and gas-phase bond dissociation energies of water and hydroxyl. *J. Phys. Chem. A*, **106**, 2727.

Scire, J.J., Jr., Yetter, R.A., and Dryer, F.L. (2001) Flow reactor studies of methyl radical oxidation reactions in methane-perturbed moist carbon monoxide oxidation at high pressure with model sensitivity analysis. *Int. J. Chem. Kinet.*, **33**, 75.

Skjøth-Rasmussen, M.S., Braun-Unkhoff, M., Naumann, C., and Frank, P. (2003) Experimental and numerical study of n-decane chemistry. In C. Chauveau and C. Vovelle (Eds.) Proceedings of the European Combustion Meeting, October 25-28, Orleans, France.

Smith, G.P., Golden, D.M., Frenklach, M., Eiteneer, B., Goldenberg, M., Bowman,C.T., Hanson, R.K., Song, S., Gardiner Jr., W.C., Lissianski, V.V., and Qin, Z. (1999) http://www.me.berkeley.edu/gri_mech/(accessed October 2003).

Stein, S.E. (1994) *NIST Standard Reference Database 25: Structure and Properties*, NIST, Gaithersburg, MD.

Wagner, P. and Dugger, G.L. (1955) Flame propagation 5. Structural influences on burning velocity—Comparison of measured and calculated burning velocity. *J. Am. Chem. Soc.*, **77**, 227.

Wang, H. and Frenklach, M. (1994) Transport-properties of polycyclic aromatic-hydrocarbons for flame modeling. *Combust. Flame*, **96**, 163.

Wang, S.Q., Miller, D.L., Cernansky, N.P., Curran, H.J., Pitz, W.J., and Westbrook, C.K. (1999) A flow reactor study of neopentane oxidation at 8 atmospheres: Experiments and modeling. *Combust. Flame*, **118**, 415.

Zeppieri, S.P., Klotz, S.D., and Dryer, F.L. (2000a) Modeling concepts for larger carbon number alkanes: A partially reduced skeletal mechanism for n-decane oxidation and pyrolysis. *Proc. Combust. Instit.*, **28**, 1587.

Zeppieri, S.P, Klotz, S.D., and Dryer, F.L. (2000b) Paper Presentations, 28th International Symposium on Combustion, July 30-August 4, 2000, Edinburgh, Scotland.

Zhao, Z. (2002) Laminar flame speed study using Particle Image Velocimetry on a stagnation flame configuration, MSE Thesis, Mechanical and Aerospace Engineering Department, Princeton University, Princeton, NJ.

Zhao, Z., Kazakov, A., and Dryer, F.L. (2004a) Measurements of dimethyl ether/air mixture burning velocities by using particle image velocimetry. *Combust. Flame*, **139**, 52.

Zhao, Z., Li, J., Kazakov, A., and Dryer, F.L. (2004b) The initial temperature and N_2 dilution effect on the laminar flame speed of propane/air mixtures. *Combust. Sci. Technol.*, **176**, 1705.

Zheng, L., Kazakov, A., and Dryer, F.L. (2003) Experimental Study of Propene Oxidation at Low and Intermediate Temperatures, 2nd Joint Meeting of the U.S. Sections of the Combustion Institute, Chicago, IL, Paper No. A03.